[2] J. G. de Koning, R. E. Goldwasser, R. J. Hamilton, Jr., and F. E. Rosztoczy, "Fullband staggered gain Gunn effect amplification in *Ka*-band," *Proc. IEEE*, vol. 63, pp. 1371–1373, Sept. 1975.
[3] K. S. Packard, "Optimum impedance and dimension for strip transmission line," *IRE Trans. Microwave Theory Tech.*, vol. 5, pp. 244–247, Oct. 1957.
[4] S. B. Cohn, "Characteristic impedance of the shielded strip transmission line," *IRE Trans. Microwave Theory Tech.*, vol. MTT-2, pp. 52–57, July 1954.
[5] G. L. Mattheai, L. Young, and E. M. T. Jones, *Design of Microwave Filters, Impedance Matching Networks and Coupling Structures*. New York: McGraw-Hill, 1964, ch. 6.
[6] H. Bosma, "Junction circulators," in *Advances in Microwaves*, vol. 6. New York: Academic Press, 1971, p. 218.

Microwave Properties of Lithium Ferrites

JEROME J. GREEN, SENIOR MEMBER, IEEE, AND H. JERROLD VAN HOOK

***Abstract*—Low-power loss and high-power threshold properties have been measured between 3.0 and 17.2 GHz on three Li-Ti ferrite compositions of magnetizations 1250, 2250, and 3600 G. In each composition the use of cobalt resulted in a linear increase in μ_0'' and h_{crit}. Temperature measurements were performed at 9.2 GHz on the 2250-G material. An illustration of how the data might be applied is given.**

I. Introduction

In recent years the lithium–titanium system [1]–[2] has been a valuable addition to the microwave ferrite family. Through the use of titanium substitution, the magnetization can be conveniently varied between 0 and 3600 G (Fig. 1) while maintaining a high Curie temperature. Currently, the materials are made with small additions of bismuth and manganese [1]. The bismuth addition permits densification to greater than 99 percent of theoretical which is essential to achieve the low coercive force and high remanent magnetization necessary in phase shifter applications. Manganese is used to decrease the dielectric loss tangent to less than 10^{-3}. To improve peak power performance in spinels, it is traditional [3], [4] to add cobalt, and for high-average-power applications, where heating can be a serious concern, a low saturation magnetization is chosen. To achieve the lowest insertion loss and most compact device, one typically chooses the lowest cobalt level and highest saturation magnetization consistent with the peak and average power performance requirements. The choice of material is determined by the frequency of application, the peak and average power requirement, and the premium on weight and switching power. Therefore, it is desirable to know the material parameters which affect device performance of a wide variety of compositions to be able to perform the necessary tradeoffs in selecting a specific composition.

In this paper we describe the microwave properties of three basic lithium–titanium compositions which have room temperature saturation magnetizations of 1250, 2250, and 3600 G. This range of magnetizations covers applications between 5.5 to 17.0 GHz. The chemical formula for these compositions is

$$Li_{0.5+(x/2)-(z/2)}Mn_yTi_xCo_zFe_{2.5-(3x/2)-y-(z/2)}O_4$$

Manuscript received December 1, 1975; revised May 25, 1976. This work was supported in part by the U.S. Air Force Materials Laboratory, Wright-Patterson Air Force Base, under Contract F33615-72-C-1524.
The authors are with the Raytheon Research Division, Waltham, MA 02154.

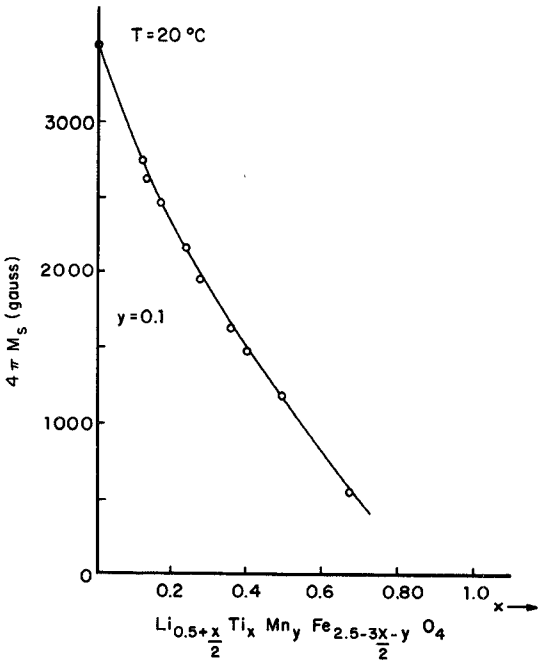

Fig. 1. Saturation magnetization versus titanium content at 20°C.

where $x = 0$ for $4\pi M_s = 3600$ G, $x = 0.26$ for $4\pi M_s = 2250$ G, and $x = 0.53$ for $4\pi M_s = 1250$ G. The Mn level in all compositions was kept at $y = 0.1$. The range in Co concentration was between $0 \leq z \leq 0.04$. Bismuth oxide (Bi_2O_3) is added at low concentrations in the original formulation of the ferrite, the purpose being to promote densification and grain growth [1] in the final sintering step. Concentrations in the range of 0.1 to 0.2 weight percent of the original batch are generally used. The Bi_2O_3 addition is essentially insoluble in the ferrite, residing primarily in boundary regions between ferrite grains where its influence on sintering kinetics is strongest. We have therefore not included Bi_2O_3 in the chemical formulation of the ferrite.

The magnetic loss parameter μ_0'' and peak power parameter h_{crit} of these three compositions has been evaluated primarily in the vicinity of 5.5, 9.2, and 17.0 GHz. Some microwave measurements were made as a function of temperature at 9.2 GHz. The experimental techniques were similar to those used for our previous papers [5], [6].

II. Temperature Dependence of Magnetization and Coercive Force

The temperature dependence of a phase shifter's differential phase shift and insertion phase is determined by the temperature performance of the hysteresis loop properties. Fig. 2 gives the dependence of the saturation magnetization upon temperature T, and Figs. 3–5 show the dependence of the remanent magnetization $4\pi M_r$ and coercive force H_c upon T. For high cobalt content there is a decrease in remanence at low temperature for the 1250- and 3600-G materials. This decrease in remanence has been previously described by Van Hook and Dionne [7] for the 3600-G composition. It is suggested that the effect is due to a change in sign of the anisotropy constant K_1 [8]. For the 1250- and 2250-G composition it has not been possible to grow single crystals so that we do not know how the anisotropy constant K_1 depends upon Co content and temperature in these compositions. We can only speculate that the same mechanism is at work in the

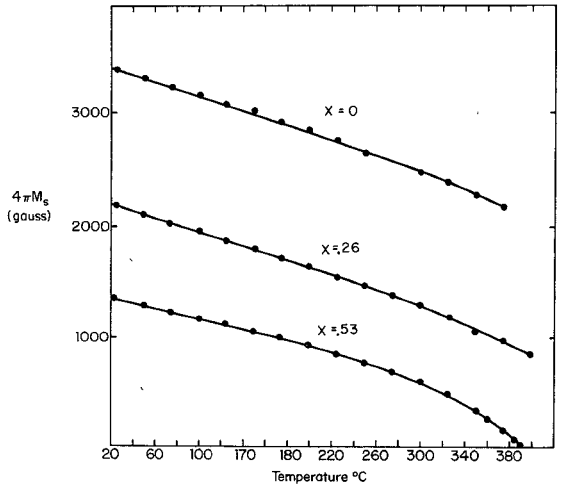

Fig. 2. Saturation magnetization versus temperature for several Li-Ti ferrites.

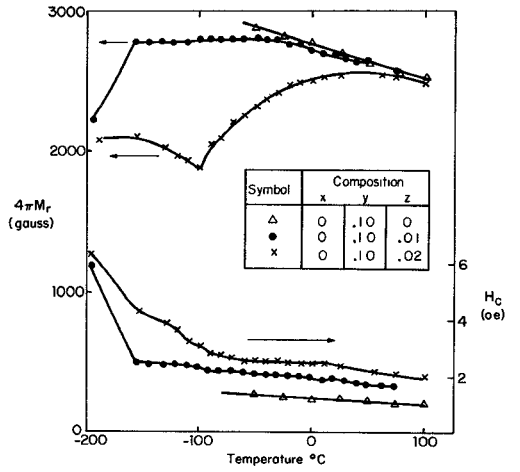

Fig. 3. Coercive force and remanent magnetization versus temperature for 3600-G materials.

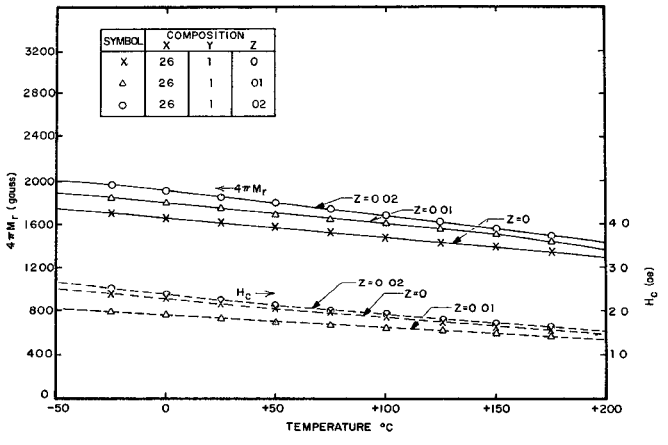

Fig. 4. Coercive force and remanent magnetization versus temperature for 2250-G materials.

$z = 0.02$, 1250-G material (Fig. 5) as is at work in the $z = 0.02$, 3600-G composition of Fig. 3.

Since the variation in device performance in the vicinity of room temperature is usually of most concern, we have listed the

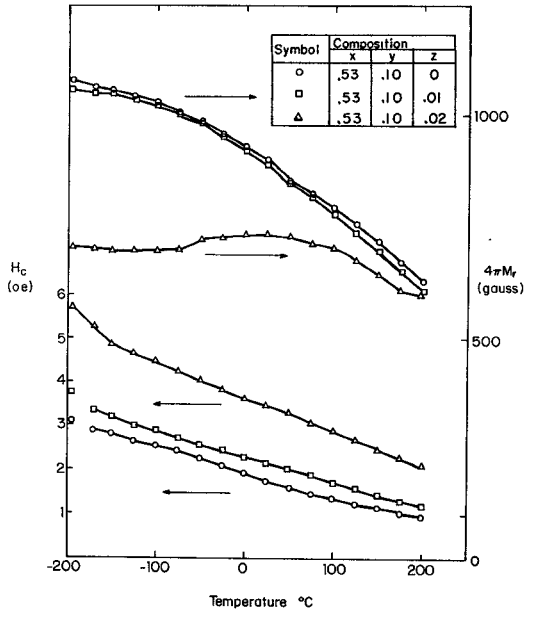

Fig. 5. Coercive force and remanent magnetization versus temperature for 1250-G materials.

TABLE I
TEMPERATURE DEPENDENCE OF HYSTERESIS PROPERTIES

z	x	y	H_c (Oe)	$\frac{dH_c}{H_c dT}$ (%/°C)	$4\pi M_s$ (gauss)	$\frac{dM_r}{M_r dT}$ (%/°C)	$4\pi M_s$ (gauss)	$\frac{dM_s}{M_s dT}$ (%/°C)
0	0	0.10	1.21	0.25	2780	0.09	3560	
0.01	0	0.10	2.05	0.20	2720	0.08	3575	0.09
0.02	0	0.10	2.50	0.20	2540	0.05	3656	
0	0.26	0.10	2.15	0.21	1600	0.12	2175	
0.01	0.26	0.10	1.80	0.18	1760	0.14	2225	0.13
0.02	0.26	0.10	2.25	0.21	1840	0.13	2300	
0	0.53	0.10	1.71	0.29	900	0.16	1235	
0.01	0.53	0.10	2.12	0.25	890	0.17	1234	0.18
0.02	0.53	0.10	3.45	0.23	735	0.08	1297	

room temperature derivatives in Table I for $4\pi M_s$, $4\pi M_r$, and H_c.

III. Magnetic Loss

The magnetic loss for a partially magnetized state such as would exist in a phase shifter or below resonance circulator can be characterized [5], [6] by a single loss parameter μ_0'', the imaginary part of the diagonal component of the permeability tensor for a demagnetized ferrite. The results for μ_0'', evaluated at three frequencies, 5.5, 9.97, and 17.3 GHz, are given in Figs. 6 and 7. We see that μ_0'' increases linearly with Co content and decreases with increasing frequency. In [6] a very useful relationship of the form $\mu_0'' = A(\gamma 4\pi M_s/\omega)^N$ was fit to the data to allow calculation as a function of frequency of the contribution of μ_0'' to phase shifter insertion loss. In our present measurements, we have been limited by high anisotropy fields to only measuring the 1250-G materials at all three frequencies. Unfortunately, additional high-frequency data would be necessary to determine the linear portions (log plot) of the μ_0'' versus $(\gamma 4\pi M_s/\omega)$ dependence. Consequently, no A or N values can be given for any materials.

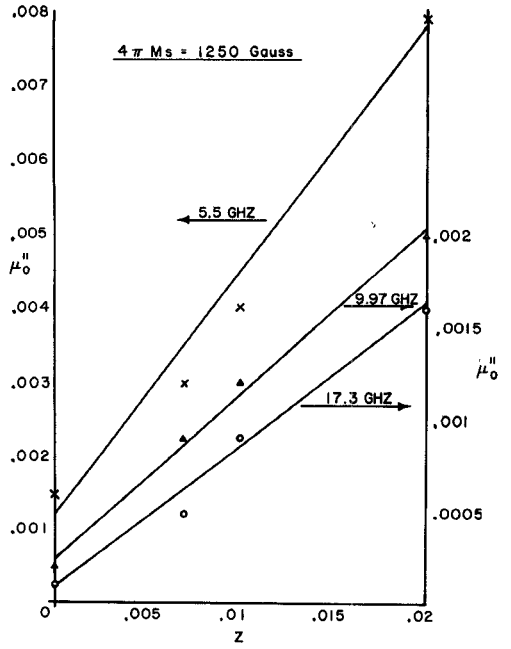

Fig. 6. Magnetic loss versus cobalt level for 1250-G material at 5.5, 9.97, and 17.3 GHz.

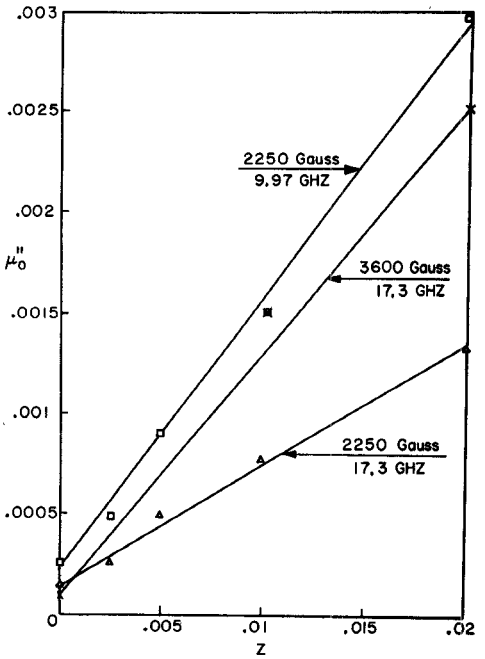

Fig. 7. Magnetic loss versus cobalt level for 2250- and 3600-G materials.

IV. High-Power Thresholds

The peak power performance can be adequately described by the parallel pump threshold for a fully magnetized sample but with the internal field approximately equal zero (i.e., external biasing field equal to the demagnetizing factor times the saturation magnetization). Fig. 8 depicts the dependence of h_{crit} upon frequency for the 1250-G composition. As in [6], we have attempted to fit these data to a relationship suitable for use in

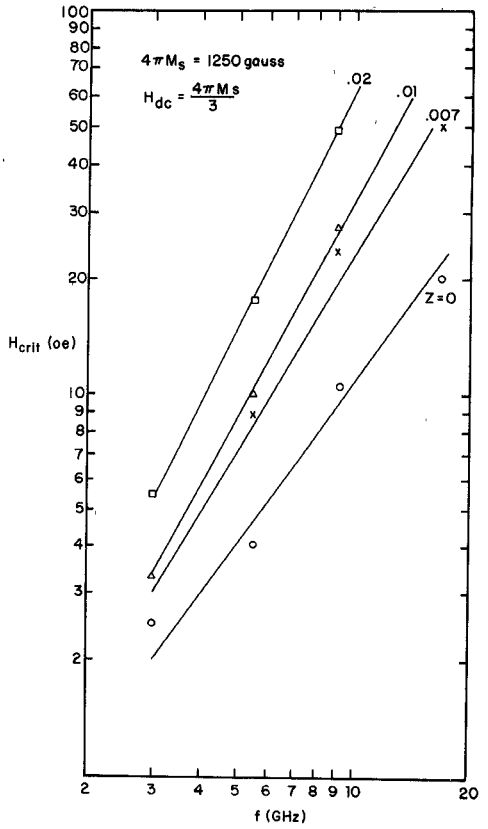

Fig. 8. Critical field versus frequency for 1250-G materials.

TABLE II

z	B (Oe)	l
0	2.53	1.31
.007	3.82	1.69
.01	4.36	1.90
.02	7.27	2.02

computer device design. It has the form

$$h_{crit} = B\left(\frac{\omega}{\gamma 4\pi M_s}\right)^{l}. \tag{1}$$

The values for B and l are given in Table II.

The results of the measurements on the 2250- and 3600-G compositions are given in Fig. 9. In this case the data have been plotted against Co level rather than frequency since there are no sufficient frequency data to determine B and l coefficients.

V. Temperature Dependence of μ_0'' and h_{crit}

Measurements were made at 9.2 GHz of μ_0'' and h_{crit} for the 2250-G composition. The dependence of μ_0'' for various Co levels is shown in Fig. 10. In Fig. 11, h_{crit} is given for these materials over the same temperature range. The data have been accumulated for two biasing fields, $H_{dc} = 4\pi M_s/3$, the field at which the sphere is magnetized but the internal field is approximately zero, and the residual field in our magnet gap which is

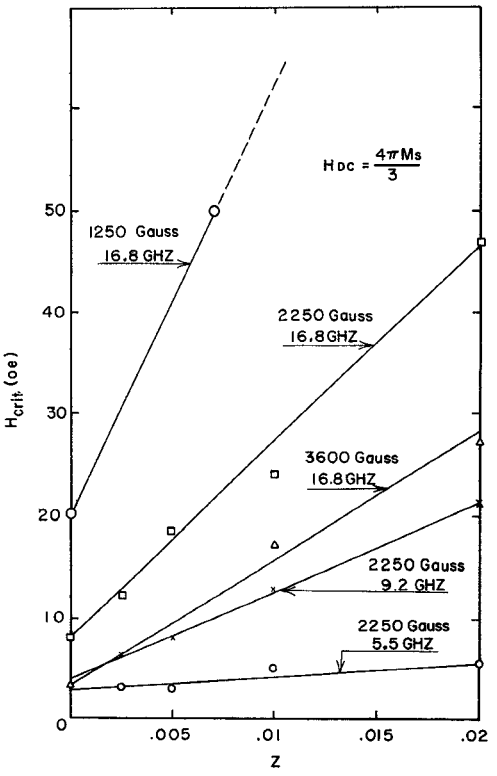

Fig. 9. Critical field versus cobalt level.

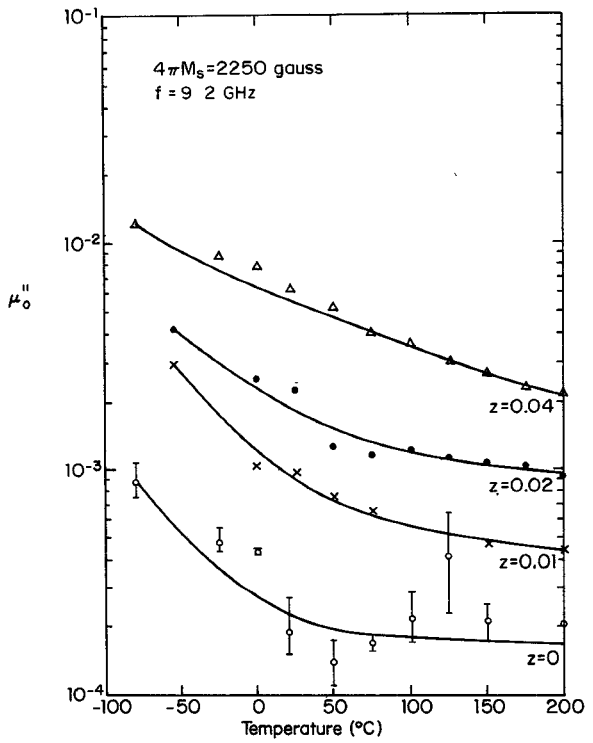

Fig. 10. Magnetic loss versus temperature for 2250-G materials at 9.2 GHz.

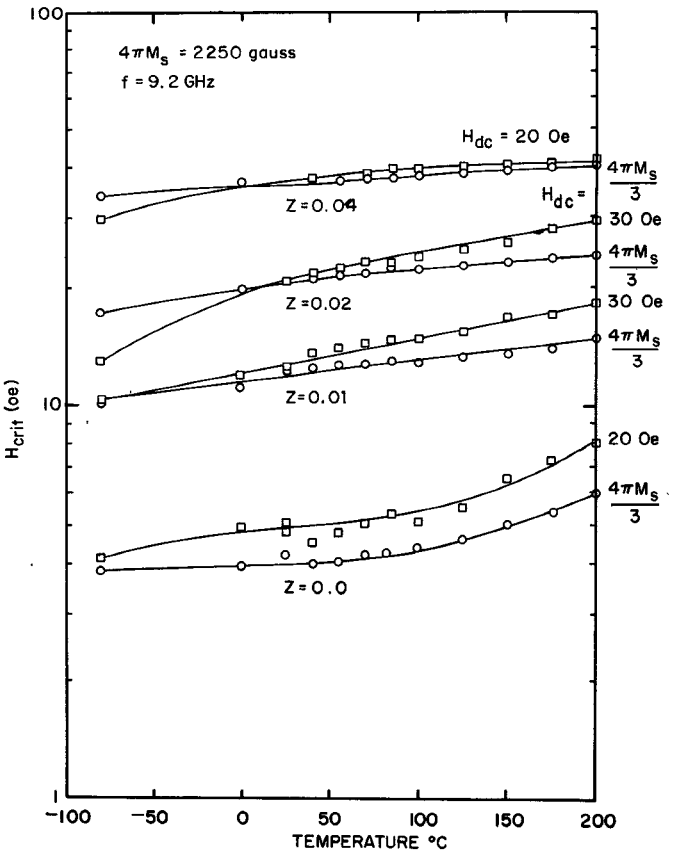

Fig. 11. Critical field versus temperature of 2250-G materials at 9.2 GHz.

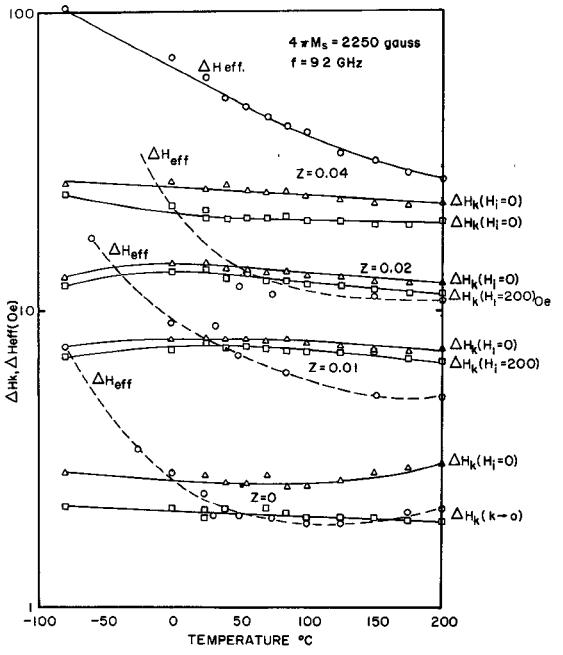

Fig. 12. Spinwave and effective linewidth versus temperature of 2250-G materials at 9.2 GHz.

20 or 30 Oe. With this latter field the sample is almost demagnetized. As can be seen from the curves, the h_{crit} values for the two fields are approximately the same, indicating that parallel pump thresholds change little throughout the partially magnetized region. While there is a significant decrease in μ_0'' with increasing temperature, there is a much more modest change of h_{crit} with temperature.

An ideal material would be one in which the loss is low and the threshold is high. Unfortunately, most techniques for increasing the peak power threshold tend to increase the loss. Since, in

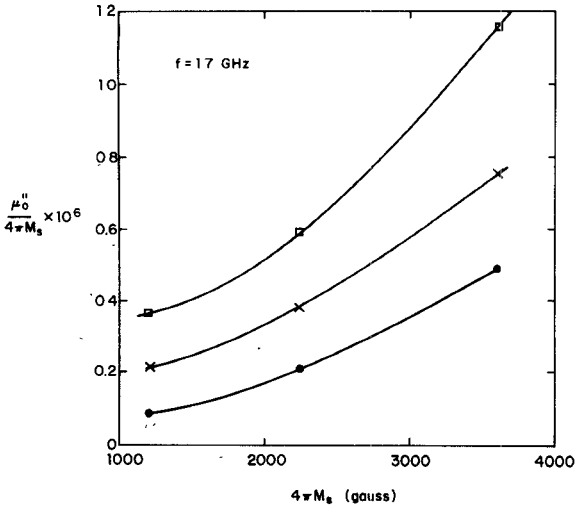

Fig. 13. Ratio $\mu_0''/4\pi M_s$ versus $4\pi M_s$.

addition to depending on the relaxation mechanisms of the material, μ_0'' and h_{crit} depend upon the angular frequency ω and $4\pi M_s$, it is illuminating to compare the fundamental relaxation parameters ΔH_{eff} and ΔH_k [6]. By dividing out the dependence upon ω and $4\pi M_s$, we can obtain a better feeling for the contest between loss and peak power threshold. In Fig. 12 we have plotted ΔH_k and ΔH_{eff} as a function of temperature for the various Co doping of the 2250-G material. There are a number of interesting features that are worth noting. ΔH_k is independent of temperature while ΔH_{eff} increases significantly at low temperature. At high temperature ΔH_{eff} is comparable to ΔH_k and in some instances is lower. This is in contrast to rare-earth relaxation in garnets where $\Delta H_{eff} = 2\Delta H_k$, which comes about from the fact that at room temperature rare-earth relaxation is proportional to frequency and the spin waves excited at high peak power have half the frequency of the uniform precession. The rapid increase in ΔH_{eff} at low temperature we suspect is due to an increase in the anisotropy field. The fact that ΔH_{eff} is comparable or lower than ΔH_k at high temperatures indicates that better ratios of peak power to insertion loss can be obtained with Co doping in these lithium–titanium compositions for high-temperature operation than with rare-earth doping in garnets.

VI. Choosing a Material

The constraints in the choice of a material to a large extent are determined by each application. For an airborne phased array, weight and therefore size are very important. In all many element arrays cost is significant which results in efforts to minimize size to reduce material cost and driver size. Low insertion loss is always desired by the system designers. If the device must handle very large average power, then there are usually few such devices per system (switches, circulators) so that size and weight are less important than in the case of an array phase shifter. The primary problem is to remove heat from the device so that it does not approach the Curie temperature of the ferrite and cease to function.

To illustrate how a device engineer might use the data presented in this article in choosing a material for the types of applications mentioned above, we have plotted in Fig. 13 the ratio $\mu_0''/4\pi M_s$. If the remanent ratio $(4\pi M_r/4\pi M_s)$ is independent of composition, a reasonable assumption in these lithium ferrite compositions, then the phase shift per unit length will be proportional to $4\pi M_s$. Therefore, for a fixed required phase shift, e.g., 360° of differential phase shift, the device length will be proportional to $(4\pi M_s)^{-1}$. Since the total magnetic insertion loss is the product of a constant (characteristic of the device cross section) with μ_0'' and device length, it is proportional to $\mu_0''/4\pi M_s$. The insertion loss for a device is the sum of mismatch loss, wall loss, dielectric material loss, and magnetic material loss with the magnetic loss being the dominant factor.

In Fig. 13 there are three curves, each for a constant h_{crit}. After deciding the value of h_{crit} necessary to meet the peak power requirements of the applications, the next decision concerns the relative importance of size, weight, and insertion loss. Going to high $4\pi M_s$ reduces size but increases magnetic insertion loss. The most common choice of $4\pi M_s$ is one that makes $\gamma 4\pi M_s/\omega$ equal to 0.6. If size and weight are very important, then a choice of $\gamma 4\pi M_s/\omega$ up to 0.7 can be considered. Above 0.7, however, μ_0'' rises very rapidly causing high insertion loss. If average power is large, then lower ratios of $\gamma 4\pi M_s/\omega$ should be considered. μ_0'' decreases so rapidly that even $\mu_0''/4\pi M_s$ decreases by going to lower $4\pi M_s$. Values of $\gamma 4\pi M_s/\omega$ less than 0.4 are infrequently considered because the device becomes long and wall losses plus dielectric material loss become dominant. If, however, very large amounts of average power must be handled and the ability to remove heat from the material is the limiting factor, then even lower values of $\gamma 4\pi M_s/\omega$ should be considered because the ability to remove heat is determined by insertion loss per unit length and not total insertion loss.

VII. Summary and Conclusions

Three basic compositions with saturation magnetization of 1250, 2250, and 3600 G have been evaluated. Measurements were made between 3.0 and 16.8 GHz on h_{crit} and between 5.5 and 17.2 GHz on μ_0''. To increase peak power performance, cobalt has been added to each basic composition resulting in a linear increase in μ_0'' and in h_{crit}. Temperature evaluation performed on the 2250-G material at 9.2 GHz indicates that at high temperature the ratio of peak power to magnetic insertion loss becomes better than that possible with the rare-earth garnets, while at low temperature this ratio degrades significantly. Plots of $\mu_0''/4\pi M_s$ versus $4\pi M_s$ at 17 GHz indicate that the magnetic insertion loss decreases with decreasing magnetization. This is particularly significant for high-average-power applications where sample heating can cause a severe problem. For applications of modest average power, the choice of the highest magnetization allowing acceptable insertion loss is a more likely choice since this reduces the volume of material and therefore phase shifter cost and weight.

References

[1] P. D. Baba *et al.*, "Fabrication and properties of microwave lithium ferrites," *IEEE Trans. Magnetics*, vol. MAG-8, p. 83, 1972.
[2] G. F. Dionne, "A review of ferrites for microwave applications," *Proc. IEE*, vol. 163, p. 777, 1975.
[3] J. J. Green and E. Schloemann, "High power ferromagnetic resonance at *X*-band in polycrystalline garnets and ferrites," *IRE Trans. Microwave Theory Tech.*, vol. MTT-8, p. 100, 1960.
[4] E. Schloemann, J. J. Green, and U. Milano, "Recent developments in ferromagnetic resonance at high power levels," *J. Appl. Phys.*, vol. 31, p. 386S, 1960.
[5] J. J. Green and F. Sandy, "Microwave characterization of partially magnetized ferrites," *IEEE Trans. Microwave Theory Tech.*, vol. MTT-22, p. 641, 1974.
[6] ——, "A catalog of low power loss parameters and high power thresholds for partially magnetized ferrites," *IEEE Trans. Microwave Theory Tech.*, vol. MTT-22, p. 645, 1974.
[7] H. J. Van Hook and G. F. Dionne, "Hysteresis loop properties of Li-ferrite doped with Mn and Co," in *AIP Conf. Proc.*, vol. 24, 1975, p. 487.
[8] M. A. Stel'mashenko and V. N. Seleznev, *Izv. VUZ fizika*, vol. 5, p. 13, 1966.